Inkjet-printed Reflection Amplifier for Increased-range Backscatter Radio

John Kimionis, Manos M. Tentzeris
School of Electrical & Computer Engineering
Georgia Institute of Technology
Atlanta, GA, 30308, USA
ikimionis@gatech.edu, etentze@ece.gatech.edu

Apostolos Georgiadis, Ana Collado
Centre Tecnologic de Telecommunicacions de Catalunya
Castelldefels 08860, Spain
{ageorgiadis, acollado}@cttc.es

***Abstract*—Building ultra large scale wireless sensor networks (WSNs) requires very low-power and low-cost sensor designs. Backscatter radio is a communication scheme that can accommodate for these two constraints, as opposed to active radio architectures. For large scale applications, backscatter communication range extension is a necessity; for this, careful tag design has to be employed, in order to minimize the tag information bit-error-rate (BER) at the reader. Conventional backscatter radio/RFID load modulators achieve reflection coefficients whose magnitude is less than unity; thus, the reflection coefficients' difference magnitude–which is directly related to the backscatter signal-to-noise ratio (SNR)–is upper bounded by $|\Delta\Gamma| \leq 2$. This is a limitation for SNR maximization, and alternative system architectures have to be exploited for load modulators. In this work, an architecture is presented that overcomes this limitation with the use of a low-power reflection amplifier, which shows a reflection coefficient greater than unity on its port. The amplify-and-reflect system proposed can be utilized to significantly increase the SNR of the backscattered signals and the uplink range of RF tags.**

***Index Terms*—backscatter radio, RFID, reflection amplifier, range increase, SNR.**

I. Introduction

Backscatter radio is a promising scheme for use in wireless sensor networks (WSNs) due to its low-power requirements and low-complexity sensor designs. Some examples of backscatter radio exploitation to form low-cost networks are [1]–[4]. Moreover, several examples exist in the literature for energy harvesting and efficient antenna design for such low-cost sensor networks [5]–[7], which supports the argument that this is an appealing technology for WSNs. It is obvious that for large scale sensing applications, backscatter communication range extension is a necessity. Recent work has shown exceptionally long communication ranges by utilizing energy-assisted tags (low energy in form of small batteries, renewable energy sources, or energy scavenging), low bitrate, and non-conventional bistatic reader architectures, where the carrier emitter is detached from the backscatter radio/RFID reader to form cells that cover large areas around many distributed carrier emitters [8], [9]. To maximize the communication range, careful tag design has to be employed, in order to minimize the tag information bit-error-rate (BER) at the reader. The work in [10] offers the constraint for BER minimization by exploiting both communication and microwave theory. It is directed that for BER minimization, $|\Delta\Gamma| \triangleq |\Gamma_1 - \Gamma_0|$ has to be maximized, where Γ_0, Γ_1 are the complex reflection coefficient values of the tag load modulation system for bits '0' and '1', respectively. This will increase the tag signal-to-noise ratio (SNR) at the reader, reducing the receiver BER; this in turn enhances the uplink range performance. Typically, load modulators consist of switches and passive components, achieving reflection coefficients Γ_0, Γ_1, whose magnitude is less than unity. This determines the upper bound $|\Delta\Gamma| \leq 2$, which is achieved for coefficients represented with two antipodal points on the Smith chart. This upper bound is a limitation for backscatter signal SNR maximization and has to be boosted upwards with the use of alternative system architectures. In this work, a system architecture is presented that overcomes this limitation with the use of a reflection amplifier. The reflection amplifier is a 1-port low-power device that shows a reflection coefficient greater than unity on its port. This amplify-and-reflect system is here utilized to significantly increase the SNR of the backscattered signals. A reflection amplifier has been proposed before for backscatter modulation, by switching the amplifier on and off [11]. A comparison is offered in this work for the achievable $|\Delta\Gamma|$ for the on-off amplifier and the proposed system, and it is shown that the complex system architecture of Fig. 1-right allows for a larger value domain for Γ_0, Γ_1. This, in turn, leaves room for more optimization of $|\Delta\Gamma|$ and the backscatter signal SNR.

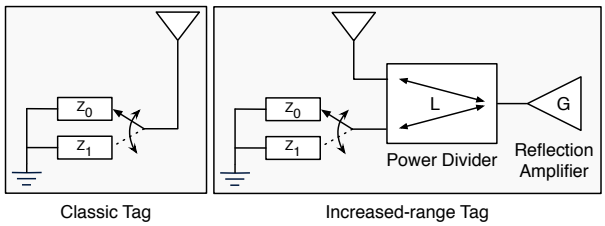

Fig. 1. Left: classic backscatter radio tag. Right: amplify-and-reflect tag.

II. System Description

The classic backscatter radio/RFID modulation mechanism is based on switching the antenna (with impedance Z_a) termination between two different loads Z_0, Z_1 (Fig. 1-left)

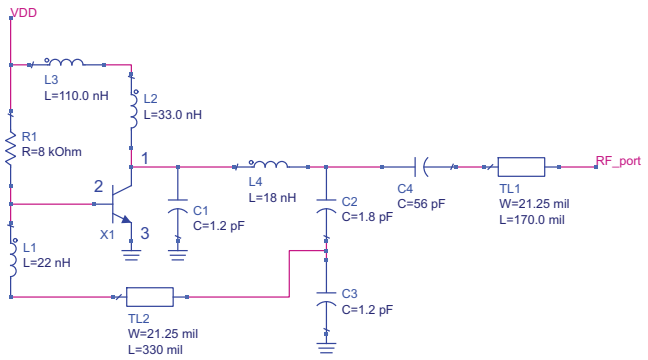

Fig. 2. Reflection amplifier schematic diagram.

[12]. In that way, two different system reflection coefficients

$$\Gamma_0 = \frac{Z_0 - Z_a^*}{Z_0 + Z_a}, \quad \Gamma_1 = \frac{Z_1 - Z_a^*}{Z_1 + Z_a} \tag{1}$$

are achieved and the amplitude and phase of the backscattered signal are affected [10]. One can then perform modulation schemes like amplitude shift keying (ASK) or binary phase shift keying (BPSK), or hybrids of them, by exploiting certain reflection coefficients and the appropriate signal model [9]. Recent work has also utilized more than two load values to achieve higher constellation modulations such as M-ary quadrature amplitude modulation (M-QAM) on backscatter radio [13]. The backscattered signal constellation is known to be directly related to the points of Γ_0, Γ_1 on the Smith chart. For example, $\Gamma_0 = -1$ and $\Gamma_1 = 1$ would correspond to BPSK modulation, since only the phase of the backscatter signal changes for the two states. This could be the case for any two antipodal points on the unitary circle (Fig. 7). Notice that for any load Z_x, the corresponding system reflection coefficient will always have magnitude $|\Gamma_x| \leq 1$.

In this work, a reflection amplifier is utilized to overcome the limitation of $|\Gamma_x| \leq 1$. The reflection amplifier is essentially a negative resistance oscillator [14]. The bias voltage of the amplifier is kept sufficiently low, so that the amplifier does not oscillate (i.e. does not generate frequencies). To interface the amplifier to an antenna and load modulator system, a 3-port network is required. For this case, a Wilkinson power divider is selected, that ideally splits/combines the power from the amplifier port to the other two ports (antenna and modulator), and keeps the antenna port isolated from the modulator port.

III. Modules

A reflection amplifier has been built according to the schematic in Fig. 2 using lumped components placed on an inkjet-printed circuit board on low-cost photo paper substrate. The dielectric characteristics of the substrate are $\epsilon_r = 2.9$, $\tan\delta = 0.045$, and its thickness is $210\mu m$. Four layers of silver nanoparticle ink have been printed to form the traces, with approximate conductivity 5×10^6 Siemens/m. The same fabrication technique has been utilized to built the Wilkinson divider. The prototypes can be seen in Fig. 3.

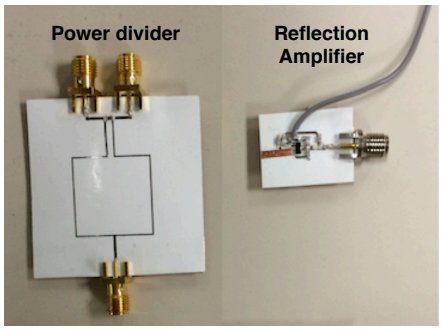

Fig. 3. Fabricated prototypes using inkjet-printing technology.

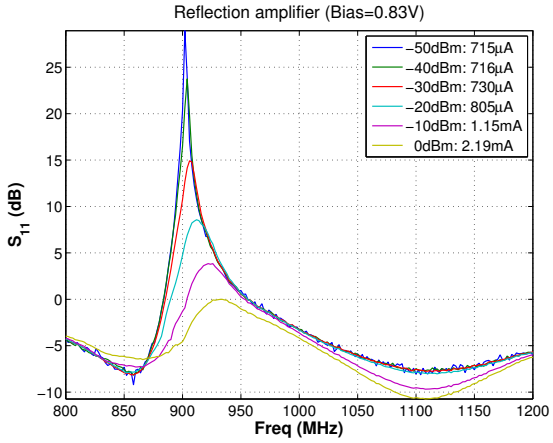

Fig. 4. Reflection amplifier measured gain for several input power levels.

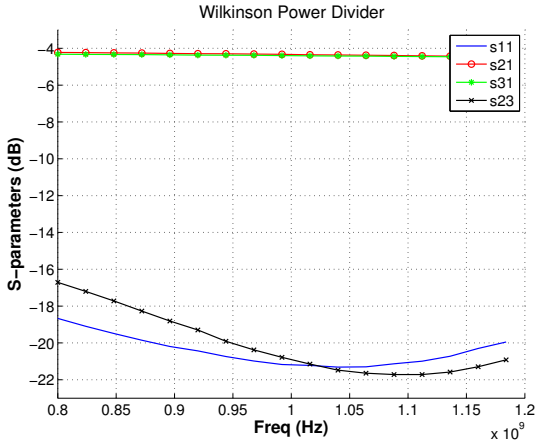

Fig. 5. Measured S-parameters for fabricated Wilkinson power divider.

The amplifier has been measured with a vector network analyzer (VNA) to characterize its reflection gain at the 900–930MHz band (Fig. 4). It can be seen that the gain increases as the input power decreases and it can go up to ∼30dB for levels below −50dBm. Its power consumption is low–under 1mA for typical received power levels below −20dBm.

The Wilkinson power divider's measured S-parameters are shown in Fig. 5. The insertion loss from port 1 to ports 2 and 3 is 4.3dB across the band, while the isolation between ports

2 and 3 is better than 19dB.

IV. Operation Analysis

The antipodal load modulator in a classic backscatter radio tag (Fig. 1-left) that maximizes $|\Delta\Gamma|$ switches between two reflection coefficients Γ_0, Γ_1. These reflection coefficients and their difference magnitude are given by

$$\Gamma_0 = -\Gamma_1 = 1\ e^{j\theta}, \tag{2}$$

$$|\Delta\Gamma| = |e^{j\theta} + e^{j\theta}| = 2, \tag{3}$$

with $\theta \in [0, 2\pi)$. This well-known case is depicted on a Smith chart in Fig. 7, where both coefficients lie on the unitary circle.

Consider now a system that consists of a reflection amplifier with power gain G directly interfaced to the antenna (as in [11]). The amplifier is switched on and off to achieve ASK backscatter modulation. When the amplifier is off, the equivalent circuit seen by the antenna port is a passive load. The system reflection coefficient will have amplitude $B \leq 1$ and arbitrary phase ϕ_0. When on, the amplifier shows a reflection voltage gain $\sqrt{G}$ and applies phase ϕ_1 to the incoming signal. Thus,

$$\Gamma_0 = B\ e^{j\phi_0}, \tag{4}$$

$$\Gamma_1 = \sqrt{G}\ e^{j\phi_1}. \tag{5}$$

Such two reflection coefficient points are shown in Fig. 8. The reflection coefficient difference amplitude is

$$|\Delta\Gamma| = |\sqrt{G}\ e^{j\phi_1} - B\ e^{j\phi_0}|. \tag{6}$$

In the best case, $|\Delta\Gamma|$ is maximized when $B = 1$ and the line that connects the two points crosses the axis origin $(0, 0)$. This is achieved when $\phi_1 = \phi_0 + \pi$. Then,

$$|\Delta\Gamma| = |\sqrt{G}\ e^{j\phi_0 + j\pi} - e^{j\phi_0}| = \sqrt{G} + 1. \tag{7}$$

Respectively, the worst case (difference is minimized) is when $B = 1$ and $\phi_1 = \phi_0$. Then,

$$|\Delta\Gamma| = |\sqrt{G}\ e^{j\phi_0} - e^{j\phi_0}| = \sqrt{G} - 1. \tag{8}$$

For the proposed system of Fig. 1-right, consider a reflection amplifier with a known complex S_{11}-parameter $S_{\text{amp}} \in \mathbb{C}$, and a power divider with known complex scattering matrix $\mathbf{S}_{\text{div}} \in \mathbb{C}^{3\times3}$. These values are obtained either by simulating the individual components or by measuring the fabricated prototypes with a lab VNA. Here, the realistic measured values are used, which account for fabrication errors, extra losses due to finite silver-ink conductivity, etc. The goal is to obtain a pair of load values $Z_0 = R_0 + jX_0$ and $Z_1 = R_1 + jX_1$ for the modulator that will maximize the overall reflection coefficient difference magnitude $|\Gamma_1 - \Gamma_0|$ of the system, for a given reflection amplifier and 3-port network that connects the antenna, amplifier, and modulator pieces together.

After importing the measured S-parameter blocks into a microwave simulation software, the model of Fig. 1-right is built. Two versions of the model are simulated to obtain the total reflection coefficient at the antenna terminal; one for load Z_0 that yields Γ_0, and one for load Z_1 that yields Γ_1.

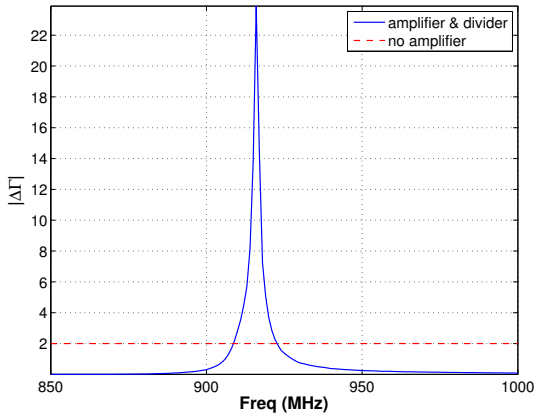

Fig. 6. Increased reflection coefficient difference magnitude around 906MHz.

A goal is then set for the software optimizer, to maximize $|\Delta\Gamma|$, at a certain frequency, or demand that $|\Delta\Gamma|$ exceeds a certain value for a frequency band. Here, the second option is preferred, since it gives the optimizer a degree of freedom of the frequency that the $|\Delta\Gamma|$ maximum will occur in the band of interest. The variables that are tuned by the optimizer are R_0, R_1, X_0, and X_1. It is anticipated that, because of the complex system architecture, several pairs of impedances may exist that satisfy the required goal. Here, an indicative pair is presented, that achieves $|\Delta\Gamma| >> 2$. The VNA-measured S-parameters are utilized; for the amplifier, the S-matrix corresponding to the -30dBm input power level is used.[1]

The optimizer goal is set to achieve a value $|\Delta\Gamma| > 20$ in the 900–920MHz band. The resulting difference magnitude as a function of frequency is shown in Fig. 6. A maximum magnitude of 23.891 is observed at 916MHz. The reflection coefficients at the antenna port are $\Gamma_0 = -0.5781 - j1.4543$ and $\Gamma_1 = 21.9297 + j6.5571$ and the corresponding modulator loads are $Z_0 = \infty$ (open) and $Z_1 = 0 + j145.403$. Notice that $|\Gamma_0| = 1.565$ and $|\Gamma_1| = 22.889$, i.e. both reflection coefficients have magnitude greater than unity, which sets them *both* outside the unitary circle of the Smith chart (Fig. 9). This is in contrast with the on-off amplifier system, where one of the two reflection coefficients always lies inside the unitary circle.

A straight comparison in terms of achieved $|\Delta\Gamma|$ between the on-off amplifier system and the proposed system can be obtained, by considering the same amplifier in both scenarios. From Fig. 4 it can be seen that for -30dBm input power, the maximum gain is 14.92dB. This corresponds to a reflection coefficient amplitude $\sqrt{G} = 5.57$. As already discussed, in the best case, the maximum coefficient difference is $\sqrt{G} + 1 = 6.57$, while in the worst case it is $\sqrt{G} - 1 = 4.57$. Thus, even with the best case for the on-off amplifier system, the proposed system is superior with achieved $|\Delta\Gamma| = 23.891$. This is the result of two things: a) both the reflection coefficients lie outside the unitary circle and incorporate phase values that

[1] System analysis can be performed for any power level in the same way.

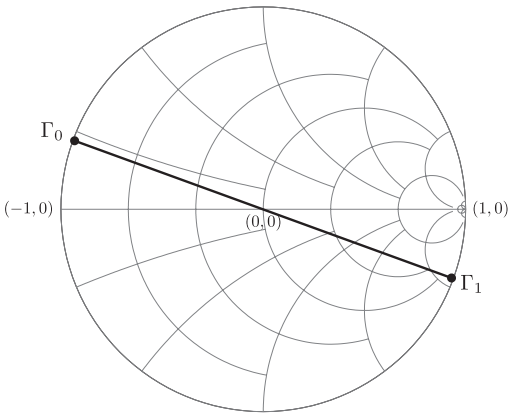

Fig. 7. For a conventional load modulator, both reflection coefficient points lie in the Smith chart. Maximum difference occurs when Γ_0 and Γ_1 lie on the circumference of the unitary circle and are diametrically opposed.

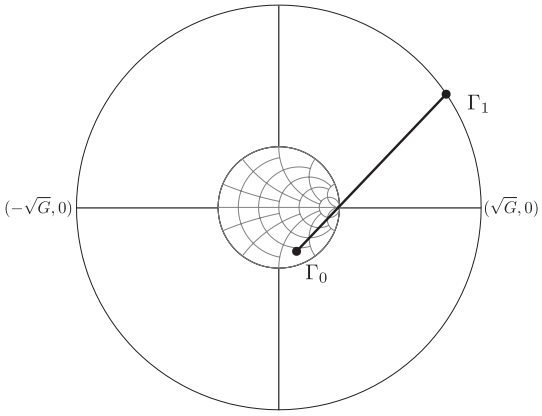

Fig. 8. When a reflection amplifier is switched on and off for load modulation, Γ_0 (off condition) lies in the Smith chart, while Γ_1 (on condition) lies away from the unitary circle (reflection gain $|\Gamma_1| > 1$).

benefit the coefficient's difference; this would be impossible with the on-off amplifier, and b) the mismatches at the Wilkinson ports of the amplifier and modulator cause infinite small reflections that are amplified, causing a big increase in the total reflection coefficient at the antenna port. Notice that 23.891 is not the *maximum* value, but rather an achieved goal for increased $|\Delta\Gamma|$. The ideal case would be that Γ_0 would have the same magnitude as Γ_1 and be diametrically opposed to it. This optimal Γ_0^{opt} point is depicted in Fig. 9.

V. Conclusion

A system architecture has been presented that can significantly increase the reflection coefficient difference magnitude for backscatter radio tags. It has been showcased that a design with a reflection amplifier, a load modulator, and a 3-port network increases the degrees of freedom for optimizing the total system reflection coefficient, compared to other systems that utilize reflection amplifiers for RF tags. This opens a whole new field for active research on backscatter communication optimization, based on careful tag microwave design. Following this direction for non-conventional tag designs and coupling it with recent work for non-conventional reader

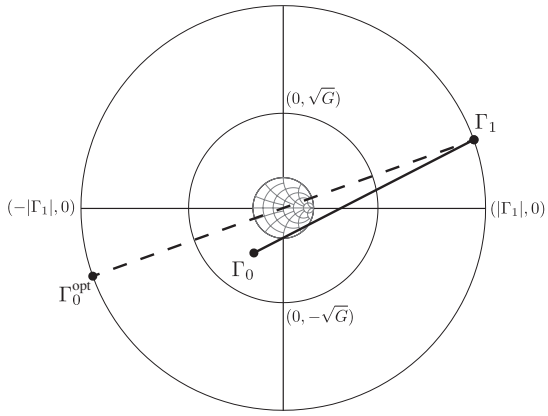

Fig. 9. For a reflection amp/power divider/load modulator system, Γ_0 and Γ_1 may both lie far from the unitary circle. In the ideal case, Γ_0 and Γ_1 are diametrically opposed.

architectures, will boost the backscatter communication range to much higher levels compared to classic RFID.

References

[1] A. Sample, D. Yeager, P. Powledge, and J. Smith, "Design of a passively-powered, programmable sensing platform for UHF RFID systems," in *Proc. IEEE RFID Conf.*, Grapevine, TX, Mar. 2007, pp. 149–156.

[2] G. Vannucci, A. Bletsas, and D. Leigh, "A software-defined radio system for backscatter sensor networks," *IEEE Trans. Wireless Commun.*, vol. 7, no. 6, pp. 2170–2179, Jun. 2008.

[3] V. Lakafosis, A. Rida, R. Vyas, L. Yang, S. Nikolaou, and M. M. Tentzeris, "Progress towards the first wireless sensor networks consisting of inkjet-printed, paper-based RFID-enabled sensor tags," *Proc. IEEE*, vol. 98, no. 9, pp. 1601–1609, Sep. 2010.

[4] E. Kampianakis, J. Kimionis, K. Tountas, C. Konstantopoulos, E. Koutroulis, and A. Bletsas, "Backscatter sensor network for extended ranges and low cost with frequency modulators: Application on wireless humidity sensing," in *Proc. IEEE Sensors 2013*, Baltimore, MD, Nov. 2013.

[5] A. P. Sample, J. Braun, A. Parks, and J. Smith, "Photovoltaic enhanced UHF RFID tag antennas for dual purpose energy harvesting," in *IEEE Intl. Conf. on RFID 2011*, Orlando, FL, Apr. 2011, pp. 146–153.

[6] A. Georgiadis and M. M. Tentzeris, "RFIDs and RFID-enabled sensors: novel applications, energy harvesting and integration challenges Workshop," in *41st European Microwave Conference (EuMC)*, Manchester, UK, Oct. 2011.

[7] R. J. Vyas, B. B. Cook, Y. Kawahara, and M. M. Tentzeris, "E-WEHP: A batteryless embedded sensor-platform wirelessly powered from ambient digital-TV signals," *IEEE Trans. Microwave Theory Tech.*, vol. 61, no. 6, pp. 2491–2505, Jun. 2013.

[8] J. Kimionis, A. Bletsas, and J. N. Sahalos, "Bistatic backscatter radio for power-limited sensor networks," in *Proc. IEEE Global Telecommunications Conference (GLOBECOM)*, Atlanta, GA, Dec. 2013, pp. 353–358.

[9] J. Kimionis, A. Bletsas, and J. N. Sahalos, "Increased range bistatic scatter radio," *IEEE Trans. Commun.*, vol. 62, no. 3, pp. 1091–1104, Mar. 2014.

[10] A. Bletsas, A. G. Dimitriou, and J. N. Sahalos, "Improving backscatter radio tag efficiency," *IEEE Trans. Microwave Theory Tech.*, vol. 58, no. 6, pp. 1502–1509, Jun. 2010.

[11] P. Chan and V. Fusco, "Bi-Static 5.8GHz RFID range enhancement using retrodirective techniques," in *41st European Microwave Conference (EuMC)*, Manchester, United Kingdom, Oct. 2011, pp. 976–979.

[12] D. M. Dobkin, *The RF in RFID: Passive UHF RFID in Practice*. Newnes (Elsevier), 2008.

[13] S. Thomas, E. Wheeler, J. Teizer, and M. Reynolds, "Quadrature amplitude modulated backscatter in passive and semipassive UHF RFID systems," *IEEE Trans. Microwave Theory Tech.*, vol. 60, no. 4, pp. 1175–1182, Apr. 2012.

[14] P. Chan and V. Fusco, "Full duplex reflection amplifier tag," *IET Microwaves, Antennas & Propagation*, vol. 7, no. 6, pp. 415–420, Apr. 2013.